Bone 125 (2019) 112–121

Contents lists available at ScienceDirect

Bone

journal homepage: www.elsevier.com/locate/bone

Full Length Article

Short-chain fatty acids and FFAR2 as suppressors of bone resorption

C.C. Montalvany-Antonucci[a,b], L.F. Duffles[a], J.A.A. de Arruda[a], M.C. Zicker[c], S. de Oliveira[d], S. Macari[e], G.P. Garlet[f], M.F.M. Madeira[g], S.Y. Fukada[h], I. Andrade Jr[b], M.M. Teixeira[i], C. Mackay[j], A.T. Vieira[i], M.A. Vinolo[d], T.A. Silva[a,*]

[a] Department of Oral Surgery and Pathology, Faculty of Dentistry, Federal University of Minas Gerais, MG, Brazil
[b] Department of Orthodontics, Faculty of Dentistry, Pontifical Catholic University, Belo Horizonte, MG, Brazil
[c] Department of Food Science, Faculty of Pharmacy, Federal University of Minas Gerais, Belo Horizonte, MG, Brazil
[d] Laboratory of Immunoinflammation, Department of Genetics, Evolution, Microbiology and Immunology, Institute of Biology, University of Campinas, Campinas, SP, Brazil
[e] Department of Pediatric Dentistry and Orthodontics, Faculty of Dentistry, Federal University of Minas Gerais, Belo Horizonte, MG, Brazil
[f] Department of Biological Sciences, School of Dentistry of Bauru, University of São Paulo, Bauru, SP, Brazil
[g] Department of Microbiology, Institute of Biological Science, Federal University of Minas Gerais, Belo Horizonte, MG, Brazil
[h] Department of Pharmacological Science, Faculty of Pharmacy, University of São Paulo, Ribeirão Preto, SP, Brazil
[i] Department of Biochemistry and Immunology, Institute of Biological Sciences, Federal University of Minas Gerais, Belo Horizonte, MG, Brazil
[j] Department of Immunology, Monash University, Melbourne, Australia

ARTICLE INFO

Keywords:
Bone remodeling
Short-chain fatty acids
FFAR2 protein

ABSTRACT

Short-chain fatty acids (SCFAs) exert a variety of immune and metabolic functions by binding to G-protein-coupled receptors, mainly free fatty acid receptor 2 (FFAR2). However, the effects of SCFAs and FFARs on bone remodeling, especially in alveolar bone, have been less explored. In this study, we investigated the influence of the SCFA/FFAR2 axis on alveolar bone. Bone samples from wild-type (WT) and FFAR2-deficient mice (FFAR2−/−) were analyzed using micro-CT, histology and qPCR. WT and FFAR2−/− animals received a high-fiber diet (HFD) reported to increase circulating levels of SCFAs. Additionally, we analyzed the effects of SCFAs and a synthetic FFAR2 agonist, phenylacetamide-1 (CTMB), on bone cell differentiation. The participation of histone deacetylase inhibitors (iHDACs) in the effects of SCFAs was further assessed *in vitro*. CTMB treatment was also evaluated *in vivo* during orthodontic tooth movement (OTM). FFAR2−/− mice exhibited deterioration of maxillary bone parameters. Consistent with this, FFAR2−/− mice exhibited a significant increase of OTM and changes in bone cell numbers and in the expression of remodeling markers. The HFD partially reversed bone loss in the maxillae of FFAR2−/− mice. In WT mice, the HFD induced changes in the bone markers apparently favoring a bone formation scenario. *In vitro*, bone marrow cells from FFAR2−/− mice exhibited increased differentiation into osteoclasts, while no changes in osteoblasts were observed. In line with this, differentiation of osteoclasts was diminished by SCFAs and CTMB. Moreover, CTMB treatment significantly reduced OTM. Pretreatment of osteoclasts with iHDACs did not modify the effects of SCFAs on these cells. In conclusion, SCFAs function as regulators of bone resorption. The effects of SCFAs on osteoclasts are dependent on FFAR2 activation and are independent of the inhibition of HDACs. FFAR2 agonists may be useful to control bone osteolysis.

1. Introduction

Short-chain fatty acids (SCFAs) are metabolic products generated by oral and gut microbiota fermentation of non-digestible polysaccharides [1]. SCFAs, mostly acetate, butyrate and propionate, achieve their function by binding to G-protein-coupled receptors (GPCRs) [1–6], FFAR2, FFAR3, GPR18 and GPR109A, or by inhibiting histone deacetylases (HDACs) [7]. GPCRs are expressed in different cell types, including neutrophils, epithelial cells, peripheral blood mononuclear cells, adipocytes and – as recently discovered – in osteoclast precursors [3,6,8,9].

SCFAs participate in various systemic events, such as body energy balance, gastrointestinal motility and inflammatory response [2,3,8,10–12]. These metabolites have been reported to potentiate or attenuate the inflammatory and immune response, depending on the pathological condition [11,13,14]. Patients with chronic and aggressive

* Corresponding author at: Department of Oral Surgery and Pathology, Universidade Federal de Minas Gerais, Av. Antonio Carlos, 6627, room 3204, Belo Horizonte, MG CEP: 31270-910, Brazil.
E-mail address: tarcilia@ufmg.br (T.A. Silva).

https://doi.org/10.1016/j.bone.2019.05.016
Received 18 January 2019; Received in revised form 30 April 2019; Accepted 13 May 2019
Available online 14 May 2019

periodontitis had increased levels of SCFAs in their gingival crevicular fluid [15,16]. Remarkably, when these patients were treated, the inflammatory parameters were reduced and the concentration of SCFAs returned to basal levels [16]. No effects of SCFAs have been previously tested in conditions of noninfectious bone resorption such as mechanically induced resorption. In this model, there is an acute transient inflammation and exacerbation of the bone remodeling process by increasing bone resorption and formation [17]. This fact makes this model suitable for investigating new pathways that might interfere with bone turnover.

The effects of SCFAs on bone metabolism have been recently associated with gut microbiota disturbances [9,18–21]. As demonstrated, SCFA supplementation in antibiotic-treated mice restores bone mass [19] and prevents menopausal and inflammation-induced bone loss [21]. One potential mechanism linking SCFAs and bone remodeling is the fact that SCFAs interfere with calcium and magnesium absorption [20,22] and augment bone mineral density and the mechanical strength of femurs [22]. Moreover, SCFAs are able to affect the formation of osteoclasts [9,21,23] and osteoblasts [24]. Considering the scarcity of studies in the literature linking SCFAs and bone – especially regarding alveolar bone – our research investigated the effects of SCFAs and FFAR2 on bone remodeling. Potential mechanisms were further explored *in vitro*.

2. Material and methods

2.1. Animals and experimental protocols

Male GPR43/FFAR2 gene-deficient (FFAR2−/−) mice were produced as previously described [25], backcrossed onto the C57BL/6 background for 10 generations and maintained in the animal facilities of Universidade Federal de Minas Gerais (UFMG), Belo Horizonte, Brazil. Wild-type (WT) C57BL/6 mice (8–12 weeks) were obtained from the center of animal care of UFMG. Animals were treated according to the regulations of the Institutional Ethics Committee (257/2014). Age- and gender-matched mice were divided into groups in order to evaluate bone phenotype in steady-state conditions or bone remodeling induced by the orthodontic tooth movement (OTM) model. Bone phenotype was also evaluated in mice fed a high-fiber diet (HFD). At the end of the experimental time, samples of maxillae, femur, vertebrae, blood and adipose tissue, as well as feces samples were collected.

2.2. Mechanically induced bone remodeling

Alveolar bone remodeling was induced by OTM, as previously described [17]. Briefly, a nickel-titanium (Ni-Ti) 0.25 × 0.76 mm coil spring (Lancer Orthodontics, San Marcos, CA, USA) was bonded between the right maxillary first molar and the maxillary incisors and a force of 0.35 N was exerted in a mesial direction. The left side (without the orthodontic coil) was used as control. The amount of OTM (μm) was determined on day 12 by measuring the distance between the cementum–enamel junction of the first and second molars using micro-computed tomography (micro-CT).

To better understand the *in vivo* effects of SCFAs, WT mice under OTM were treated by daily local injections of a FFAR2 agonist (CTMB-Phenylacetamide-1) (20 mM) or vehicle (DMSO diluted in PBS) in the right vestibular gingiva (3 μL) plus palatal mucosa (7 μL) for 7 days. Maxillae were collected after 6 days of OTM for micro-CT analysis.

2.3. Micro-CT

Maxillary alveolar bone, femurs and vertebrae were fixed in 10% neutral buffered formalin for 48 h and scanned using a micro-CT system (Skyscan 1172 X-ray microtomography; Skyscan, Aartselaar, Belgium). The calibration was carried out with known density calcium hydroxyapatite phantom (Skyscan, Aartselaar, Belgium). High-resolution scans with an isotropic voxel size of 18 μm were acquired (50 Kv, 0.5 mm aluminum filter, 0.5° rotation angle). A regular and uniformly shaped region of interest was used as a contouring method to delineate the region of interest (ROI) in the furcation area of the first molar root and vertebrae; and an irregular and anatomic ROI adjacent to the endocortical boundary was used in the metaphyseal region of distal femurs [26]. The tissue was analyzed to determine bone mineral density (BMD g/cm^{-3}), bone volume (BV mm^3), percent bone volume/tissue volume (BV/TV %), trabecular bone pattern factor (Tb.Pf mm), trabecular thickness (Tb.Th μm), trabecular number (Tb.N mm), and trabecular separation (Tb.Sp μm). Alveolar bone crest (ABC) loss was measured by determining the area between the cemento-enamel junction (CEJ) and the ABC (ABC-CEJ μm^2) in three-dimensional images of the first, second and third molars (Fiji – National Institute of Health, Bethesda, MD, USA).

2.4. Histopathological analysis

Maxillae were decalcified in 14% ethylenediaminetetraacetic acid, pH 7.4, and embedded in paraffin. Four-μm thick sections of the first and second molars with their mesial and distal-buccal root, the third molar and adjacent structures, including the periodontal ligament and alveolar bone, were selected for bone cell counting.

Osteoblasts were counted on the distal side of the distal buccal root of the maxillary first molar. For this process, sections were stained with Masson's trichrome for osteoblast identification. Osteoclasts were identified as tartrate-resistant acid phosphatase (TRAP, Sigma-Aldrich, Saint Louis, MO, USA)-positive multinucleated cells located on the bone surface and were counted on the medial side of the distal buccal root of the maxillary first molar. TRAP staining was performed according to the manufacturer's instructions. At least three serial vertical sections containing the above mentioned structures were evaluated for each animal for each analysis.

2.5. Femur mechanical analysis

Mechanical properties of maximum load were determined by testing right femurs to fracture in a universal testing machine (EMIC, DL 10000, Curitiba, PR, Brazil) equipped with a load cell of 500 N, and TESC software, version 13.4 (EMIC). Bones were tested by the three-point bending flexural test, with force applied at a speed of 1.0 mm/min in the anterior-posterior direction. The gap between the two points was 8 mm and a 2 N preload was used for 30 s.

2.6. Total RNA extraction and qPCR

For qPCR, total RNA was extracted from (1) periodontal ligament and surrounding alveolar bone from the maxillary first molars; (2) bone marrow-derived osteoclasts and osteoblasts; (3) intraperitoneal neutrophils (positive controls of GPCR expression). Extraction was done using RNeasy Mini Kit (Qiagen, Valencia, CA, USA). The integrity of RNA samples was checked by analyzing 1 μg total RNA on a 2100 Bioanalyzer (Agilent Technologies, Santa Clara, CA, USA). Complementary DNA was synthesized using a Quanti TectRT kit (Qiagen). qPCR was performed in a Viia7 instrument (LifeTechnologies, Carlsbad, CA, USA) using inventoried optimized TaqMan primer/probe sets (Invitrogen, Carlsbad, CA, USA) for murine samples, analyzed with the RT2 profiler software (SABiosciences, Qiagen) for normalizing target gene expression levels by constitutive genes (GAPDH, ACTB, Hprt1) and the respective controls. Gene expression levels were represented as fold change relative to control.

2.7. High-fiber diet (HFD)

The HFD was formulated as previously described [13]. Mice were maintained on an HFD (AIN93M with the addition of pectin (10%) and

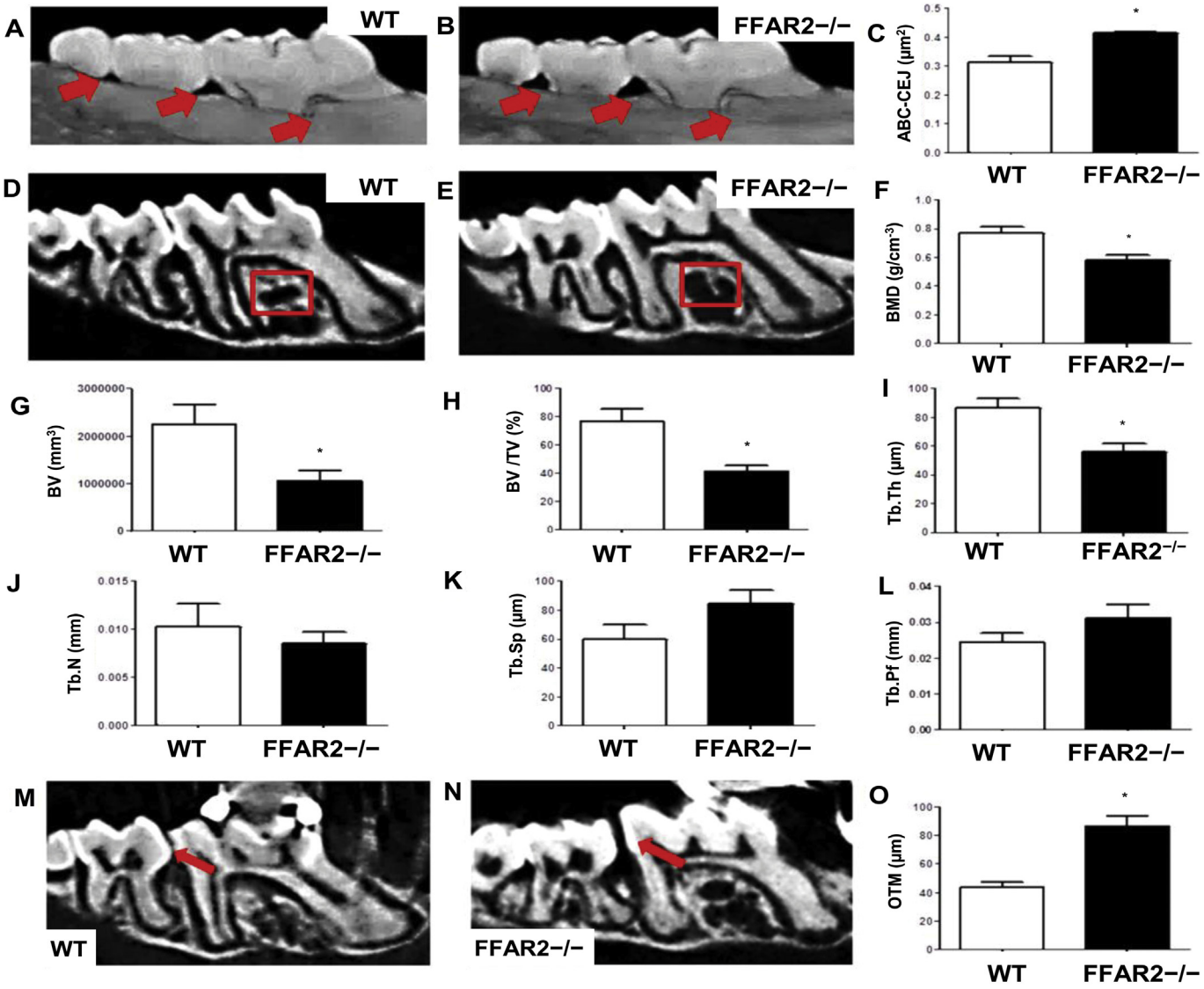

Fig. 1. Representative images of the alveolar bone crest-cement enamel junction (ABC-CEJ) (A-B) and maxillary bone parameters (D-E) in WT and FFAR2−/− mice. Quantification of the area (mm^2) of ABC-CEJ (C). (D-E) Micro-CT bone parameters (BMD, BV, BV/TV, Tb.Th, Tb.N, Tb.Sp, and Tb.Pf) of WT and FFAR2−/− mice (G-L). Representative images and quantification of the orthodontic tooth movement (OTM) in WT and FFAR2−/− mice (M-O). In A-B, red arrows indicate the alveolar bone crest. In D-E, red squares represent the analyzed area. In M-N, red arrows indicate the gap between the first and second upper molars after OTM. Seven mice were used per group. Data were expressed as mean ± SEM. * $p < 0.05$. (For interpretation of the references to colour in this figure legend, the reader is referred to the web version of this article.)

a normal or chow diet (AIN93M) for 17 days. Samples of white adipose tissue of WT and FFAR2−/− mice were then collected. Samples of epididymal (EAT), retroperitoneal (RAT), inguinal (IAT) and mesenteric (MAT) white adipose tissue were weighed and the adiposity index was calculated using the following formula: (EAT + RAT + MAT) / body weight in grams) × 100. Fecal pellets were also collected for SCFAs quantification as previously described [27].

2.8. Elisa

Serum was obtained from WT and FFAR2−/− mice to determine the concentration of adiponectin, resistin, leptin and chemerin. Adipokines were detected using ELISA kits (R&D Systems Europe, Abington, UK) according to the manufacturer's instructions. Serum from WT and FFAR2−/− mice under control and HFD conditions were assayed for the detection of C-terminal telopeptides of type I collagen (CTX-I) using Serum CrossLaps® CTX-I ELISA (IDS Immunodiagnostic Systems Holdings, Tyne & Wear, UK).

2.9. Osteoclast cultures

Bone marrow cells (BMCs) were obtained from the femur and tibia of WT and FFAR2−/− mice. For osteoclast differentiation, BMCs were incubated in minimum essential medium alpha (MEM α, no nucleosides) (Thermo Fisher Scientific, Waltham, MA, USA) supplemented with 10% heat-inactivated fetal bovine serum (FBS) (Gibco; Thermo Fisher Scientific) and 30 ng/mL soluble macrophage colony-stimulating factor (M-CSF) (R&D Systems Europe) for 3 days. After this time, adherent cells were collected and seeded in a 96 well plate. A number of 2×10^4 cells/well were stimulated with M-CSF and 10 ng/mL RANKL (R&D Systems Europe). Just after cell seeding, the following treatments were added: (1) acetate, butyrate and propionate, separately, at 10 μM or 15 μM; (2) SCFA mix containing acetate (10 μM), butyrate (5 μM) and propionate (10 μM); (3) FFAR2 agonist (CTMB- Phenylacetamide-1) (Merck Millipore, Burlington, MA, USA) at 2 μM; (4) iHDACs (Entinostat - ET; RGFP966 - RG; CI994 – Ci9; PCI34051 - PCI) and Vorinostat (SAHA, Selleck, Houston, TX, USA) at 2 μM for 2 h prior to

SCFA treatment. The iHDACs and CTMB were diluted in DMSO, and the vehicle was also tested. After 24 h, the medium was replaced and the osteoclast cell culture continued with only M-CSF and RANKL stimuli for another 3 days. On day 7, cells were collected for qPCR analysis or were fixed for TRAP staining. The number of TRAP-positive (TRAP +) cells with > 3 nuclei was determined by counting the number of cells in 10 fields per well at 40× magnification.

Each experiment was performed twice and independent cell viability tests were conducted for all experimental groups using the MTT (3-(4,5-dimethylthiazol-2-yl)-2,5-diphenyltetrazolium bromide) assay. Osteoclast activity was tested by seeding BMCs in an osteoassay surface 96 well plate (Corning, NY, USA) for the measurement of resorption-pit formation as previously described [17].

2.10. Osteoblast cultures

BMCs from WT and FFAR2−/− mice were cultured in a medium containing 10% FBS, 100 μM L-ascorbic acid, 10 nM dexamethasone, and 5 nM glycerophosphate. At day 21, the formed calcium deposits were quantified using a 1% alizarin solution. Calcium deposits were dissolved in 10% acetic acid and methanol and absorbance was evaluated at 490 nm. At day 21, cells were also collected for qPCR.

2.11. Statistical analysis

Data are presented as mean ± standard error of the mean. Differences between groups were determined by one-way ANOVA followed by the Newman–Keuls post-hoc test or by two-way ANOVA followed by the Bonferroni *post-hoc* test. $p \leq 0.05$ was considered statistically significant.

3. Results

3.1. Lack of FFAR2 induces alveolar bone loss and deteriorates maxillary microarchitecture

In a steady-state condition, FFAR2−/− mice showed a significant increase in the distance from the cementum–enamel junction to the alveolar bone crest (Fig. 1A-C) and deterioration of maxillary bone parameters (BMD, BV, BV/TV, Tb.Th) (Fig. 1D-I) when compared to WT mice. No significant difference was detected in the Tb.N, Tb.Sp or Tb.Pf parameters (Fig. 1J-L). When FFAR2−/− mice were submitted to mechanically induced bone remodeling, an increased amount of OTM was observed compared to WT mice (Fig. 1M-O).

3.2. FFAR2−/− mice showed increased numbers of osteoclasts and reduced numbers of osteoblasts in alveolar bone

Consistent with deteriorated maxillary bone parameters, FFAR2−/− mice showed an increase of osteoclasts (Fig. 2A, B) and a reduction of bone-lining osteoblasts (Fig. 2C, D) in tooth-surrounding bone under steady state condition. Noteworthy, mechanical force was not able to induce in FFAR2−/− the increase in bone cells observed for WT mice. Thus, under mechanical force, the number of osteoclasts was similar in both animal groups and osteoblasts were significantly reduced in FFAR2−/− mice in relation to WT mice (Fig. 2B, D).

3.3. Bone cells express short-chain fatty acid (SCFA) receptors and mechanical force augments their expression

Considering the impact of FFAR2 on bone, we next evaluated the expression of GPCRs in alveolar bone under OTM and in cultured bone cells. Our findings revealed that while expression of FFAR2 and GPR18 was significantly stimulated during OTM (Fig. 3A-B), no significant changes in the expression of FFAR3 or GPR109A were observed (Fig. 3C, D).

Differentiated osteoclasts and osteoblasts expressed FFAR2 (GPR43), FFAR3 (GPR41), GPR18 and GPR109A. FFAR2 was the most expressed receptor in both cells. The expression of GPCRs in bone cells was lower compared with neutrophils (gray line) used as positive control (Fig. 3E, F).

Considering the participation of SCFAs in the inflammatory response, we also evaluated the expression of TNF-α, IL-6 and IL-1β cytokines in alveolar bone (Fig. 3G-I). We observed that, under steady state conditions, WT and FFAR2−/− mice showed similar expression of all targets analyzed. OTM significantly increased the expression of inflammatory molecules in both animal groups. The expression of TNF-α and IL-1β was similar when comparing WT and FFAR2−/− mice submitted to OTM (Fig. 3G-I). However, IL-6 expression was significantly lower in FFAR2−/− than in WT mice (Fig. 3H).

3.4. Alveolar bone of FFAR2−/− mice exhibited changes in expression of osteoblastic and osteoclastic markers

FFAR2−/− mice exhibited apparently disrupted homeostasis in the expression of remodeling markers, which is consistent with alveolar bone phenotype (Fig. 4A-F). A significant increase of RANKL (Fig. 4A), MMP13 (Fig. 4B), OPG (Fig. 4C) and a reduction of RANK expression (Fig. 4D) were observed in FFAR2−/− mice. ALP expression was increased in the alveolar bone of FFAR2−/− compared with WT mice (Fig. 4E). The osteoblast marker RUNX2 was similarly expressed in WT and FFAR2−/− mice (Fig. 4F).

3.5. The HFD partially reversed alveolar bone loss in FFAR2−/− mice

The HFD used in our experiments has been reported to enhance the levels of various SCFAs, including acetate [28]. Regarding the analysis of SCFAs in feces, data were as follows: (WT control, the mean of acetate was 5.80 ± 2.04 μM/g, the mean of butyrate was 2.23 ± 0.20 μM/g, and the mean of propionate was 2.76 ± 0.37 μM/g; for 2); (WT HFD, the mean of acetate was 7.52 ± 1.70 μM/g, the mean of butyrate was 2.25 ± 0.52 μM/g, and the mean of propionate was 2.75 ± 0.26 μM/g; for 3); (FFAR2−/− mice control, the mean of acetate was 5.92 ± 0.63 μM/g, the mean of butyrate was 2.10 ± 0.44 μM/g, and the mean of propionate was 3.30 ± 0.69 μM/g; (FFAR2−/− mice HFD, the mean of acetate was 5.77 ± 2.24 μM/g, the mean of butyrate was 2.16 ± 0.58 μM/g, and the mean of propionate was 3.08 ± 0.72 μM/g). HFD intake did not impact the bone phenotype in WT mice (Fig. 4G, H, K, L, O, P). The amount of horizontal alveolar bone loss was not modified by the HFD ingestion (Fig. 4I, J, M, N, Q). In contrast, the HFD partially reversed the bone loss observed in FFAR2−/− mice, as demonstrated by the increase in BMD and BV/TV values (Fig. 4O-P).

Although no changes were seen in the bone architecture of WT mice fed the HFD, these mice showed a reduced expression of RANKL, MMP13 and RANK (Fig. 4A-C) and an augmented expression of OPG and ALP in alveolar bone (Fig. 4C, E). In contrast, FFAR2−/− mice fed the HFD showed no significant change in the expression of these markers when compared with FFAR2−/− mice fed a control diet (Fig. 4A-F). Additionally, serum CTX-I levels were similar in both animal groups and were not significantly affected by HFD (Fig. 4R).

No significant changes in FFAR2 (GPR43), GPR18 or FFAR3 (GPR41) expression were observed (Fig. 4S-U). Nevertheless, FFAR2−/− mice fed the HFD showed increased expression of GPR109A in alveolar bone compared with WT fed the same diet (Fig. 4V).

Systemically, WT animals fed the HFD exhibited a reduction in body weight and adiposity, while no effects were seen in FFAR2−/− mice fed the HFD compared to FFAR2−/− mice receiving the control diet. FFAR2−/− mice receiving the control diet had reduced body weight and adiposity compared to WT mice fed the control diet (Appendix Fig. 1A-B).

No changes in the serum concentration of adiponectin or chemerin

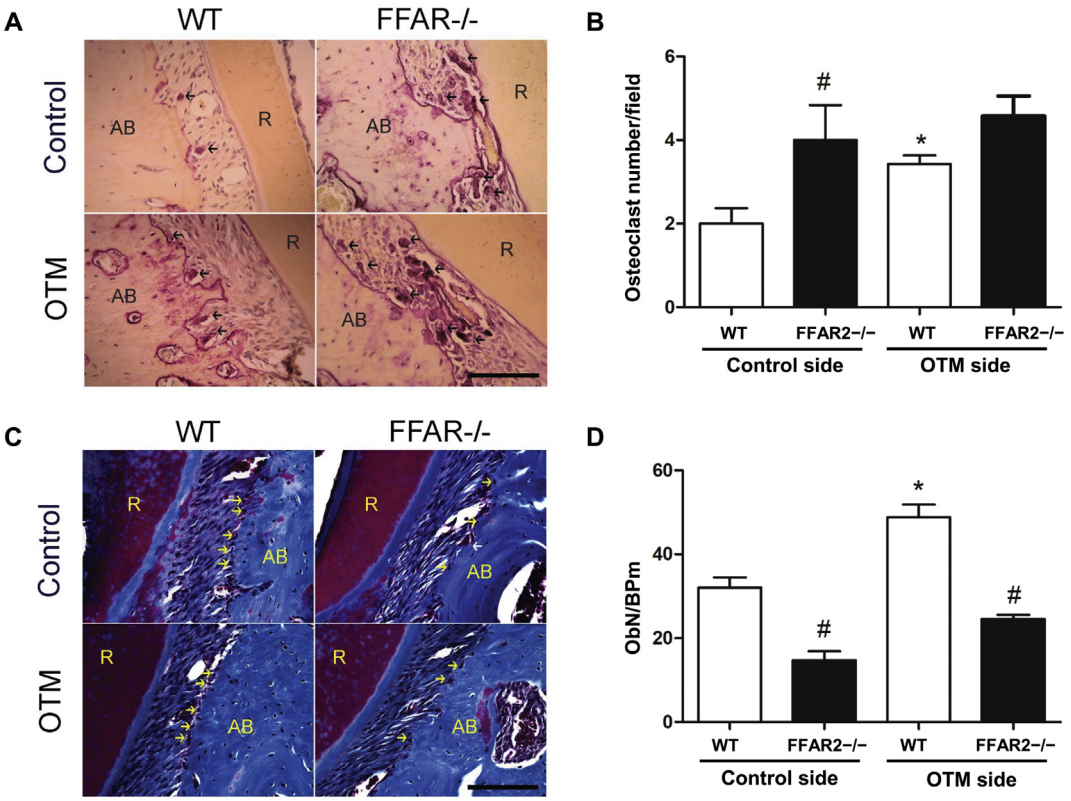

Fig. 2. Bone cell counts in tooth surrounding bone. Representative images and quantification of TRAP-positive osteoclasts counted on the maxillary bone in WT and FFAR2−/− groups on the control side and under orthodontic tooth movement (OTM) (A-B). Representative images and quantification of the bone lining osteoblasts counted on the maxillary bone of WT and FFAR2−/− mice on the control and OTM side (C-D). (AB) alveolar bone; (R) root; (ObN/BPm) osteoblast numbers/bone perimeter. In A, black arrows indicate osteoclasts. In B, yellow arrows indicate osteoblasts. Scale bar = 100 μm. Seven mice were used per group. Data were expressed as mean ± SEM. * $p < 0.05$ comparing OTM with control side. # $p < 0.05$ comparing WT and FFAR2−/− mice in same experimental condition. (For interpretation of the references to colour in this figure legend, the reader is referred to the web version of this article.)

were seen comparing all groups (Appendix Fig. 1C-D). Resistin levels were higher in FFAR2−/− mice compared to WT mice, independently of diet type (Appendix Fig. 1E), while leptin was only significantly augmented in FFAR2−/− mice receiving the HFD compared to WT under the same condition (Appendix Fig. 1F).

3.6. Femur and vertebra bone parameters in FFAR2−/− mice

Different from maxillae, most femurs parameters were similar in FFAR2−/− and WT mice (Appendix Fig. 2), except for the augmented bone volume (Appendix Fig. 2D) and maximum load mechanical property seen in FFAR2−/− mice (Appendix Fig. 2H). For the vertebrae, FFAR2−/− mice showed a slight reduction of the following parameters: BMD, BV/TV and Tb.N (Appendix Fig. 3A-C, E, G). Other bone parameters were similar for both animal groups (Appendix Fig. 3D, F, H).

3.7. BMCs derived from FFAR2−/− showed increased differentiation into osteoclasts and were responsive only to butyrate

To investigate potential mechanisms linking SCFAs and bone, we analyzed the *in vitro* differentiation of BMCs. We found increased osteoclast formation in BMCs from FFAR2−/− mice compared to WT mice under the same experimental conditions (Fig. 5A-C). We also tested the effects of SCFAs on osteoclasts derived from FFAR2−/− mice and observed that only butyrate was able to reduce osteoclastogenesis (Fig. 5B, C). Cell viability was not significantly affected by SCFA treatment in any experiment (data not shown).

3.8. Treatment with SCFAs reduced osteoclast differentiation

Acetate, butyrate and propionate treatment at 10 μM negatively impacted osteoclast differentiation in BMCs from WT mice (Fig. 5D-F). Similar effects were seen at a dose of 15 μM (data not shown). The SCFA mix also reduced osteoclast formation without compromising cell activity (Fig. 5D, F, H). Moreover, no significant difference in resorption-pit formation was seen after SCFA treatment. (Fig. 5H, I). No changes in osteoblast differentiation were seen when comparing mineralized nodule formation from BMCs of WT and FFAR2−/− mice (Fig. 5J, K).

3.9. Effects of SCFAs on osteoclasts are dependent on FFAR2 activation

Since we observed that SCFAs reduced osteoclast differentiation, we evaluated if the mechanism involved FFAR2 activation or HDAC inhibition. An FFAR2 agonist (CTMB) promoted a significant reduction of osteoclast differentiation (Fig. 5D, F) and function (Fig. 5H-I). In contrast, pretreatment of SCFA mix-stimulated osteoclasts with iHDACs Entinostat (ET), RGFP966 (RG), CI994 (CI), PCI34051 (PCI) and Vorinostat (SAHA) did not significantly modify the effects of SCFAs (Fig. 5E, G). No significant impact of iHDAC treatment alone on osteoclast differentiation was observed. CTMB and iHDAC effects on cell viability were checked and no significant alteration was observed (data not shown).

3.10. Local treatment with an FFAR2 agonist reduces mechanically induced bone remodeling

As CTMB was able to significantly reduce osteoclast formation and resorption *in vitro*, we tested if local treatment, *i.e.*, injection around the

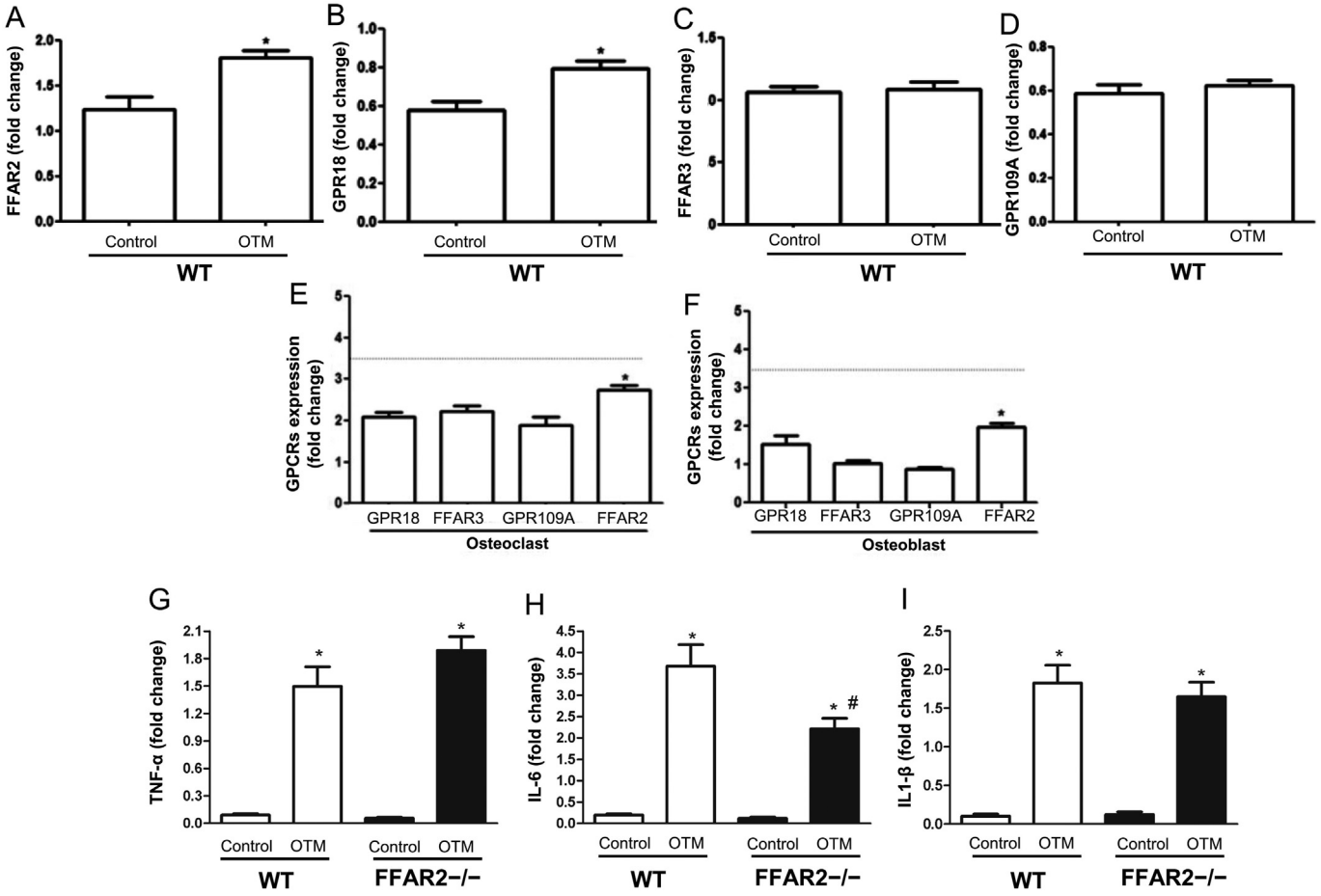

Fig. 3. Expression of GPCRs in alveolar bone and bone cells. Expression of FFAR2, GPR18, FFAR3 and GPR109A at periodontal sites submitted to orthodontic tooth movement (OTM) and controls (A-D) of WT mice. Expression of GPCRs in osteoclasts (E) and osteoblasts (F) of WT mice cultured *in vitro* for 7 and 21 days, respectively. Expression of the inflammatory mediators TNFα (G), IL-6 (H) and IL1-β (I) in alveolar bone of WT and FFAR2−/− mice under OTM and controls. Seven mice were used per group in the *in vivo* study and two mice were used per cell culture experiment. Data were expressed as mean ± SEM. * $p < 0.05$ different from control side. # $p < 0.05$ comparing WT and FFAR2−/− mice in the same experimental condition. In E-F, * $p < 0.05$ comparing FFAR2 to other GPCRs. The dotted gray line represents mean FFAR2 expression in intraperitoneal neutrophils.

teeth, would modify bone remodeling during OTM. We obtained a significant decrease of OTM after 7 days' treatment compared with to vehicle (Fig. 6).

4. Discussion

In the current study, we demonstrated that SCFAs and FFAR2 exert key functions on alveolar bone. We showed that both osteoclasts and osteoblasts express GPCRs and this expression is increased by mechanical loading in the maxillae. FFAR2−/− mice displayed a deterioration of maxillary bone, which was partially reversed by an HFD intake. Alveolar bone of FFAR2−/− mice showed a reduction of osteoblasts, an increase of osteoclast numbers and consistent changes in bone turnover markers. In line with these findings, BMCs derived from FFAR2−/− mice showed increased differentiation into osteoclasts. Moreover, we proved that osteoclast differentiation is negatively regulated by SCFAs. The FFAR2 agonist induced effects similar to those of SCFAs on differentiation and additionally reduced osteoclast resorption, indicating that the observed phenotype is dependent on FFAR2 activation and independent of HDAC inhibition since pretreatment with iHDACs did not modify the effects of SCFA on osteoclasts. Finally, local treatment with the FFAR2 agonist was able to inhibit the *in vivo* bone remodeling induced by OTM.

SCFAs are considered to be major secondary metabolites produced as a result of the fermentation of nondigestible carbohydrates by gut bacteria [10,12,26]. After being metabolized, SCFAs are found in high concentrations in the colon (70–140 mM) and the oral cavity (11–38 mM) [18]. However, plasma SCFA concentrations are low, ranging around 1–4 μM for butyrate, 3–7 μM for propionate, and 60–150 μM for acetate [18]. Effects of SCFAs on systemic bone metabolism have been recently demonstrated [9,18–21]. Concerning alveolar bone, a possible link of SCFAs and inflammatory bone loss came from the observation of an increased concentration of these molecules in the gingival fluid of patients with periodontitis [15,16]. Here, we investigated the contribution of the FFAR2 receptor to bone alveolar remodeling. The lack of FFAR2-impacted alveolar bone phenotype was observed by an increased distance between the cementum–enamel junction and the alveolar crest and the worsening of bone parameters. In parallel, we observed an increase in RANKL and MMP13 that was consistent with increased resorption in detriment of bone formation. These results clearly demonstrated that, by interfering with SCFAs/FFAR2, we can negatively impact bone health. It seems that these effects involve an imbalance of bone cells recruitment and the RANKL pathway.

Some recent evidence explains bone modulation by SCFAs, *i.e.*, (1) SCFAs reduce environmental pH by solubilizing complexation of mineral. The levels of circulating calcium increase and calcium is absorbed by bone, increasing bone mineral density [18,20,22,29]; (2) SCFAs indirectly regulate bone remodeling by modulating circulating insulin-like growth factor-1 [19]; (3) SCFAs directly reduce osteoclast

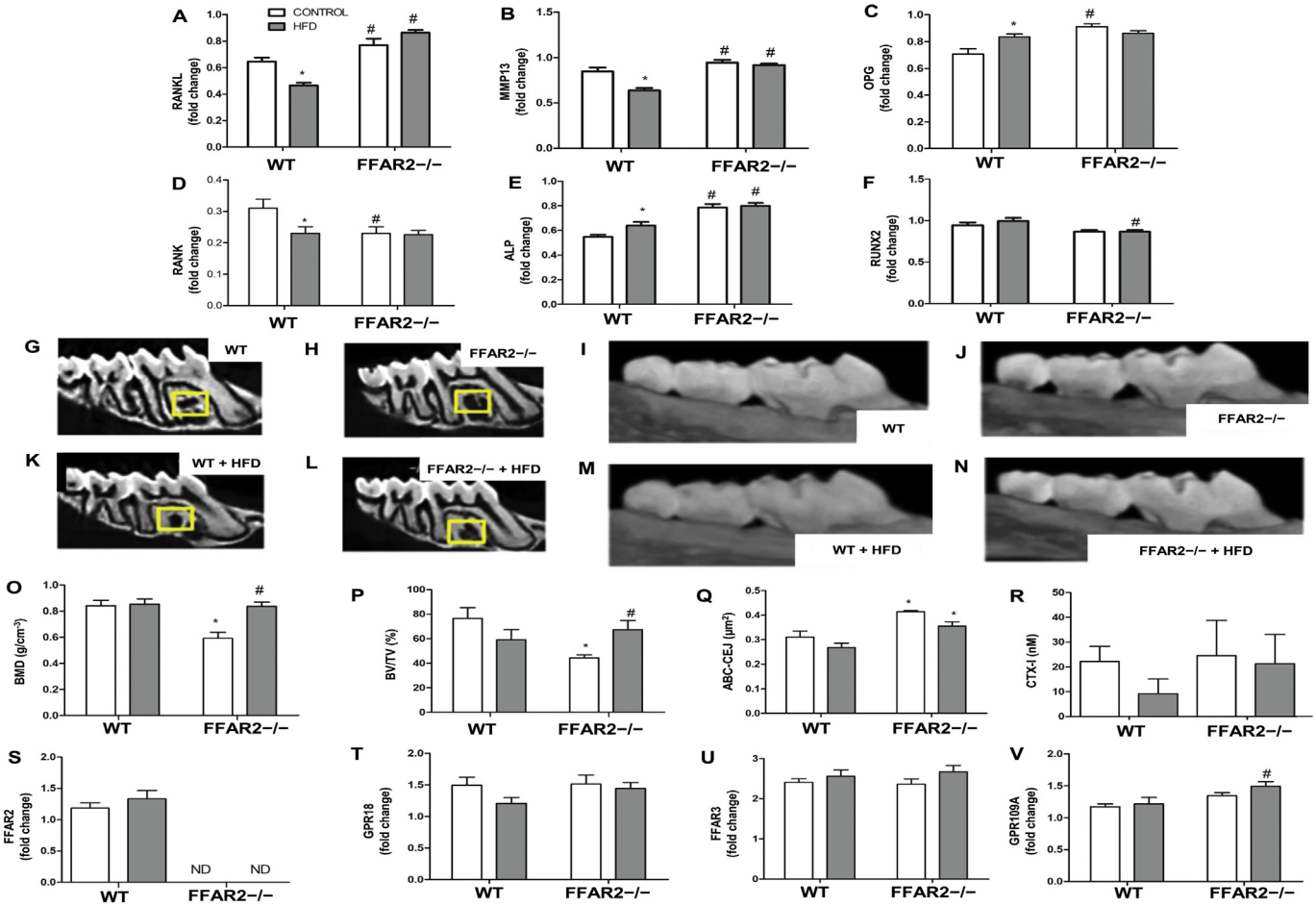

Fig. 4. Effects of a high-fiber diet (HFD) on alveolar bone. Expression of the bone turnover markers RANKL, MMP13, OPG, RANK, ALP, and RUNX2 in alveolar bone of WT and FFAR2−/− mice. Micro-CT representative images of maxillary alveolar bone microarchitecture (G, H, K, L) and of alveolar bone crest loss (I, J, M, N) in WT and FFAR2−/− mice. BMD and BV/TV parameters in alveolar bone (O-P) and amount of the area of the alveolar bone crest-cement enamel junction (ABC-CEJ) (Q). Serum concentration of C-terminal telopeptides of type I collagen (CTX-I) (R). Expression of GPCRs FFAR2, GPR18, FFAR3, and GPR09A in alveolar bone of WT and FFAR2−/− mice fed the control diet or HFD (S-V). In G, H, K, M, yellow squares represent the analyzed area. Seven mice were used per group. Data were expressed as mean ± SEM. * $p < 0.05$ comparing control diet with HFD for the same animal group. # $p < 0.05$ comparing WT and FFAR2−/− mice on the same diet. (For interpretation of the references to colour in this figure legend, the reader is referred to the web version of this article.)

formation [9,21,23] *via* GPCR-dependent effects [9] and by interfering with osteoclast energy metabolism [21]; and (4) SCFAs affect osteoblast differentiation and osteoprotegerin secretion [24]. In the present study, we additionally show that FFAR2−/− mice exhibited increased levels of circulating resistin, a fact that may contribute to the deleterious effects of FFAR2 deficiency on bone since previous data demonstrated that this deficiency is negatively correlated with BMD *in vivo* [30]. In addition, circulating levels of resistin are 2-fold higher in menopausal women and are positively associated with osteoporotic fractures [31]. We also detected a reduced expression of IL-6 in alveolar bone of FFAR2−/− mice submitted to mechanical force. Although IL-6 activates osteoclastogenesis [32], its deficiency is associated with low bone mass and reduced osteoblast numbers [33]. Thus, the contribution of this cytokine to the observed bone phenotype deserves further investigation.

The direct effects of SCFAs on bone are supported by the demonstration of GPCR expression in osteoclast precursors [9]. Accordingly, we found that all tested GPCRs (FFAR2, FFAR3, GPR18 and GPR109A) were expressed in both differentiated osteoclasts and osteoblasts. Among the GPCRs analyzed, FFAR2 was mostly expressed in both bone cells, perhaps suggesting a hierarchy of this receptor. Importantly, mechanical force resulted in increased FFAR2 and GPR18 expression in alveolar bone, which may represent a regulatory mechanism to prevent force-induced osteolysis. Accordingly, FFAR2−/− showed increased rates of force-induced bone resorption compared to WT mice. In line with these findings, we determined that an acetate, butyrate, propionate and SCFA mix was effective in reducing osteoclast differentiation. Interestingly, while osteoclast function was not compromised by SCFAs, the CTMB significantly reduced resorption-pit formation. Previous studies [9,21] have demonstrated a dose-dependent reduction of osteoclast differentiation when butyrate and propionate were administered in culture. As opposed to our results, others [9,21] did not find a significant impact of acetate on osteoclasts. Consistently, FFAR2−/− derived BMCs showed an increased differentiation into osteoclasts, and an impairment of osteoclastogenesis was observed when FFAR2−/− osteoclasts were treated with butyrate. This result suggests that the effect of butyrate on osteoclasts is independent of FFAR2. Indeed, the affinity of SCFAs for FFAR2 varies among them (acetate = propionate > butyrate), and butyrate has a higher affinity for FFAR3 and GPR41 than for FFAR2 [1–6].

Besides having direct effects by binding to GPCRs [1–6], SCFAs also affect cell function through their activity as HDAC inhibitors [7]. HDACs are considered to be specific enzymes that control gene expression by removing acetyl groups from histone and non-histone protein complexes [34]. Inhibition of HDACs is an important pathway regulating proinflammatory gene expression and osteoclast formation [34,35]. We did test if the effects of SCFAs on osteoclasts are dependent on iHDACs. Our results revealed that iHDAC pretreatment did not

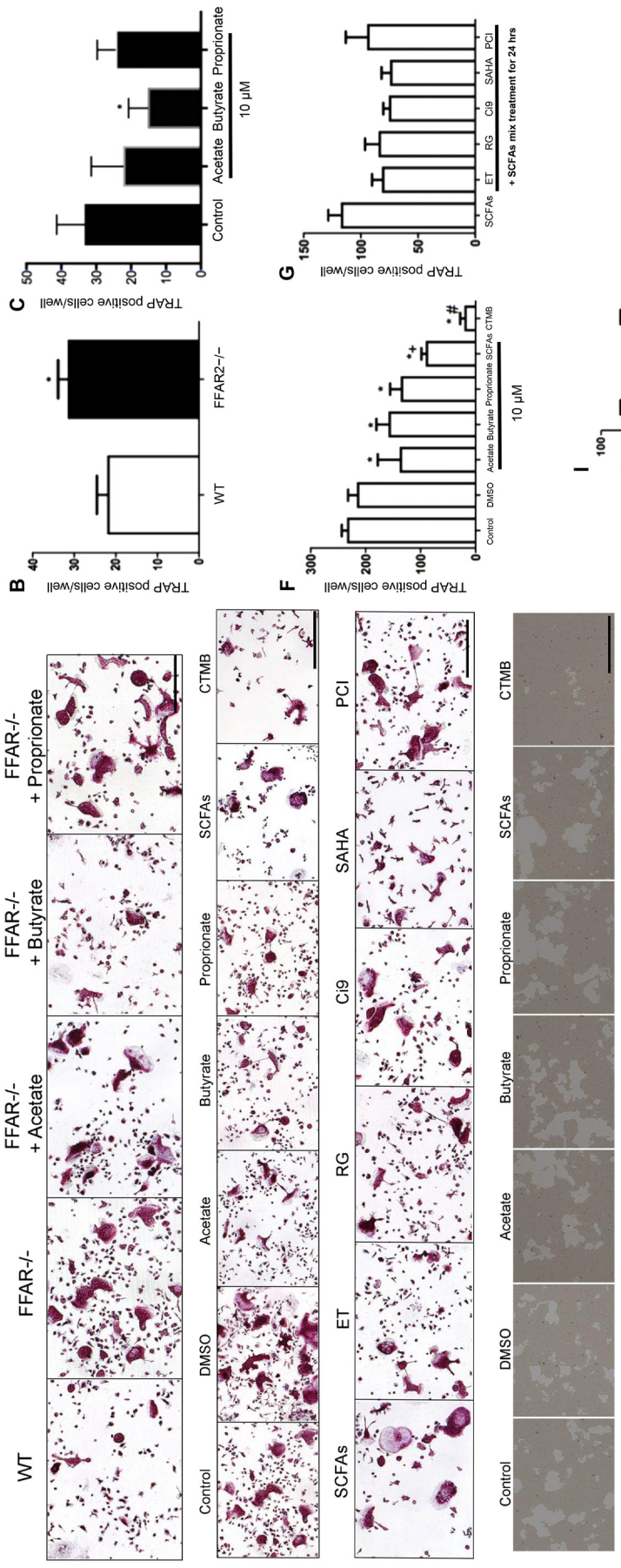

Fig. 5. Effects of FFAR2/SCFAs on bone cells *in vitro*. TRAP-positive osteoclasts formed from BMCs derived from WT and FFAR2 −/− mice (A-B). Osteoclasts from FFAR2 −/− mice after SCFA (acetate, butyrate and propionate at 10 μM) treatment (A, C). Osteoclast differentiation (D, F) and activity (H-I) after treatment with SCFAs (acetate, butyrate, propionate and SCFAs mix at 10 μM concentration) and an FFAR2 agonist (CTMB) (D-E). Effects of iHDAC (Entinostat-ET, RGFP966-RG, CI994-CI, Vorinostat-SAHA, and PCI34051-PCI) pretreatment on SCFA-stimulated osteoclasts (E, G). Mineralized deposit formation by osteoblasts differentiated from BMCs of WT or FFAR2 −/− mice (J-K). Each experiment was performed twice and data were expressed as mean ± SEM. Seven mice were used per group in the *in vivo* study and two mice were used per cell culture experiment. $^{*}p \leq 0.05$ compared to the respective controls. $^{\#}p \leq 0.05$ compared to SCFA-treated cells. $^{+}p \leq 0.05$ compared to propionate-treated cells. Scale bar = 200 μm.

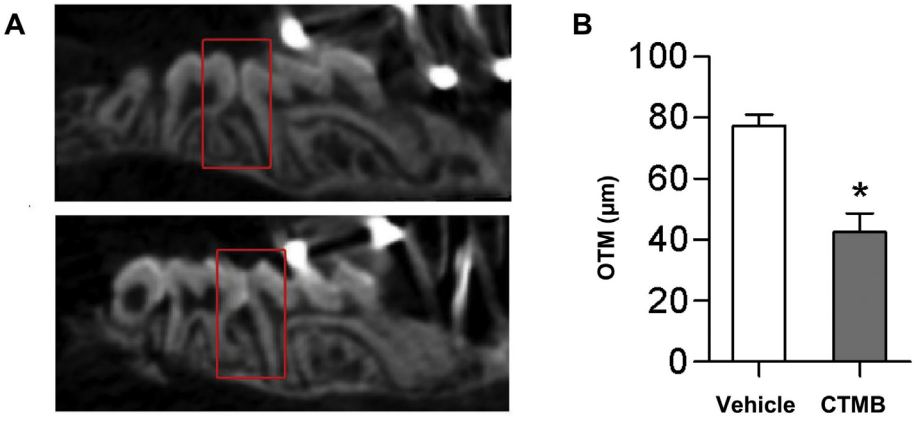

Fig. 6. Local treatment with a FFAR2 agonist (CTMB) reduced orthodontic tooth movement (OTM). Micro-CT representative images (A) and amount of OTM after treatment with vehicle (DMSO diluted in PBS) or CTMB (20 mM) (B). The red square indicates the gap between the first and second upper molars after OTM. Seven mice were used per group. Data were expressed as mean ± SEM. * $p < 0.05$ different from PBS treatment. (For interpretation of the references to colour in this figure legend, the reader is referred to the web version of this article.)

modify the effects of SCFAs, suggesting that the mechanism by which SCFAs inhibit osteoclast formation is independent of HDAC inhibition.

The HFD used in our experiments has been reported to enhance the levels of various SCFAs, including acetate [28]. Although we did use the same experimental conditions, we observed a slight increase of acetate in feces of WT mice receiving HFD. The causes for this apparent discrepancy may be 1) method of SCFAs quantification, we used for analysis gas chromatography instead of liquid chromatography; 2) analysis of feces instead of serum. Here, no significant modification of bone parameters was detected in WT mice, a fact that could be attributed to the short period of HFD administration. However, WT mice fed an HFD showed a significant reduction in the osteoclastic markers RANK, RANKL and MMP13 and an increase of ALP and OPG expression. These results may indicate that SCFAs interfere with bone turnover markers, apparently favoring bone formation. These mice also showed a reduction of body weight and adiposity that might have contributed to changes in bone markers. In FFAR2−/− mice fed an HFD, the deleterious effects on alveolar bone were partially reversed as demonstrated by the increase in key bone parameters. These results suggest the participation of GPCRs other than FFAR2 linking SCFAs and bone. Interestingly, there was an increased expression of GPR109A in FFAR2−/− mice fed an HFD and this receptor was shown to be important for the effects of SCFAs on bone [9]. FFAR2−/− mice fed an HFD also showed leptin secretion that may have been related to the improvement of bone parameters since leptin enhances osteoblast differentiation and inhibits bone resorption [36]. Although the effects of longer exposure to an HFD need to be further analyzed, our data may provide a starting point for clinical studies on nutritional intervention for patients with alveolar bone disorders.

In contrast to its pronounced effect on osteoclasts, FFAR2 deletion had no significant impact on osteoblast differentiation *in vitro*. Little information regarding the effects of SCFAs on osteoblasts is available beyond the finding that butyrate increases osteoblast differentiation [24]. We observed a reduced osteoblast population in the alveolar bone of FFAR2−/− mice under steady state conditions. Moreover, OTM did not induce an increase of the osteoblast population as seen for WT mice. This may suggest that changes in osteoclasts account for the major effects of SCFAs on bone, but the participation of osteoblasts needs to be further explored.

In contrast to the maxillae, we observed better bone parameters and mechanical properties in the femurs of FFAR2−/− mice. In line with these findings, Yan et al. [9] reported a modest improvement of trabecular bone volume in female GPR109a−/− mice. The authors partially attributed these findings to increased serum levels of procollagen type I N-terminal propeptide (P1NP), a serum marker of bone formation, suggesting that osteoblasts might be positively modulated in these animals [9]. In addition, there were no significant changes in the level of the bone resorption marker CTX-I, suggesting that osteoclast activity in GPR109a−/− mice was similar to controls [9]. Systemic alteration such as the reduction in body weight and adiposity index [37] observed in FFAR2−/− mice could also contribute to improving the femur parameters. In contrast, the vertebrae of FFAR2−/− mice exhibited worse parameters. In our study, the opposite findings observed in alveolar bone and vertebrae compared to femurs may be attributed to a different local and systemic effect of FFAR2 and SCFAs on bone homeostasis.

In conclusion, we have provided evidence for the regulatory role of SCFAs acting *via* FFAR2 on bone resorption. The direct effects of SCFAs on osteoclasts seem to be independent of HDAC inhibition. Of clinical relevance, the current study highlights that FFAR2 agonists might be a useful strategy for the control of bone loss.

Supplementary data to this article can be found online at https://doi.org/10.1016/j.bone.2019.05.016.

Author roles

C.C. Montalvany-Antonucci, L.F. Duffles, T.A. Silva, A.T. Vieira, M.A. Vinolo and S. Macari contributed to the conception and design of the study, to data acquisition, analysis, and interpretation, and drafted and critically revised the manuscript. J.A.A. de Arruda, G.P. Garlet, M.F.M. Madeira, S.Y. Fukada, I. Andrade Jr., M.M. Teixeira, S. de Oliveira, and C. Mackay contributed to the conception and design of the study and to data acquisition, and drafted and critically revised the manuscript. All authors gave final approval and have agreed to be accountable for all aspects of the work.

Declaration of Competing Interest

None.

Acknowledgments

This study was supported by the Coordination for the Improvement of Higher Education Personnel (CAPES, Finance Code 001) and the Brazilian National Council for Scientific and Technological Development (CNPq). The authors declare no potential conflicts of interest with respect to the authorship and/or publication of this article.

References

[1] N. Takahashi, Oral microbiome metabolism: from “who are they?” to “what are they doing?”, J. Dent. Res. 94 (2015) 1628–1637, https://doi.org/10.1177/0022034515606045.
[2] L.B. Bindels, E.M. Dewulf, N.M. Delzenne, GPR43/FFA2: physiopathological relevance and therapeutic prospects, Trends Pharmacol. Sci. 34 (2013) 226–232, https://doi.org/10.1016/j.tips.2013.02.002.
[3] L.M. Cornal, M.L. Mathai, D.H. Hryciw, A.J. McAinch, The therapeutic potential of GPR43: a novel role in modulating metabolic health, Cell. Mol. Life Sci. 70 (2013) 4759–4770, https://doi.org/10.1007/s00018-013-1419-9.
[4] V. Katritch, V. Cherezov, R.C. Stevens, Structure-function of the G protein-coupled

receptor superfamily, Annu. Rev. Pharmacol. Toxicol. 53 (2013) 531–556, https://doi.org/10.1146/annurev-pharmtox-032112-135923.
[5] I. Kimura, D. Inoue, K. Hirano, G. Tsujimoto, The SCFA receptor GPR43 and energy metabolism, Front. Endocrinol. (Lausanne). 5 (2014) 85, , https://doi.org/10.3389/fendo.2014.00085.
[6] Z. Ang, J.L. Ding, GPR41 and GPR43 in obesity and inflammation - protective or causative? Front. Immunol. 7 (2016) 28, , https://doi.org/10.3389/fimmu.2016.00028.
[7] L.C. Boffa, G. Vidali, R.S. Mann, V.G. Allfrey, Suppression of histone deacetylation in vivo and in vitro by sodium butyrate, J. Biol. Chem. 253 (1978) 3364–3366.
[8] R.O. Corrêa, A. Vieira, E.M. Sernaglia, M. Lancellotti, A.T. Vieira, M.J. Avila-Campos, H.G. Rodrigues, M.A.R. Vinolo, Bacterial short chain fatty acid metabolites modulate the inflammatory response against infectious bactéria, Cell. Microbiol. 19 (2017) 1–14, https://doi.org/10.1111/cmi.12720.
[9] J. Yan, A. Takakura, K. Zandi-Nejad, J.F. Charles, Mechanisms of gut microbiota-mediated bone remodeling, Gut Microbes 9 (2018) 84–92, https://doi.org/10.1080/19490976.2017.1371893.
[10] G. den Besten, K. van Eunen, A.K. Groen, K. Venema, D.J. Reijngoud, B.M. Bakker, The role of short-chain fatty acids in the interplay between diet, gut microbiota, and host energy metabolism, J. Lipid Res. 54 (2013) 2325–2340, https://doi.org/10.1194/jlr.R036012.
[11] M.H. Kim, S.G. Kang, J.H. Park, M. Yanagisawa, C.H. Kim, Short-chain fatty acids activate GPR41 and GPR43 on intestinal epithelial cells to promote inflammatory responses in mice, Gastroenterology 145 (2013) 396–406 e1–10 https://doi.org/10.1053/j.gastro.2013.04.056.
[12] C.K. Chakraborti, New-found link between microbiota and obesity, World J. Gastrointest. Pathophysiol. 6 (2015) 110–119, https://doi.org/10.4291/wjgp.v6.i4.110.
[13] A.L.M. Silveira, A.V.M. Ferreira, M.C. de Oliveira, M.A. Rachid, L.F. da Cunha Sousa, F. Dos Santos Martins, A.C. Gomes-Santos, A.T. Vieira, M.M. Teixeira, Preventive rather than therapeutic treatment with high fiber diet attenuates clinical and inflammatory markers of acute and chronic DSS-induced colitis in mice, Eur. J. Nutr. 56 (2017) 179–191, https://doi.org/10.1007/s00394-015-1068-x.
[14] J. Park, C.J. Goergen, H. HogenEsch, C.H. Kim, Chronically elevated levels of short-chain fatty acids induce T cell-mediated ureteritis and hydronephrosis, J. Immunol. 196 (2016) 2388–2400, https://doi.org/10.4049/jimmunol.1502046.
[15] L. Qiqiang, M. Huanxin, G. Xuejun, Longitudinal study of volatile fatty acids in the gingival crevicular fluid of patients with periodontitis before and after nonsurgical therapy, J. Periodontal Res. 47 (2012) 740–749, https://doi.org/10.1111/j.1600-0765.2012.01489.x.
[16] R. Lu, H. Meng, X. Gao, L. Xu, X. Feng, Effect of non-surgical periodontal treatment on short chain fatty acid levels in gingival crevicular fluid of patients with generalized aggressive periodontitis, J. Periodontal Res. 49 (2014) 574–583, https://doi.org/10.1111/jre.12137.
[17] I.L. Lima, S. Macari, M.F. Madeira, L.F. Rodrigues, P.M. Colavite, G.P. Garlet, F.M. Soriani, M.M. Teixeira, S.Y. Fukada, T.A. Silva, Osteoprotective effects of IL-33/ST2 link to osteoclast apoptosis, Am. J. Pathol. 185 (2015) 3338–3348, https://doi.org/10.1016/j.ajpath.2015.08.013.
[18] C.M. Weaver, Diet, gut microbiome, and bone health, Curr. Osteoporos. Rep. 13 (2015) 125–130.
[19] J. Yan, J.W. Herzog, K. Tsang, C.A. Brennan, M.A. Bower, W.S. Garrett, B.R. Sartor, A.O. Aliprantis, J.F. Charles, Gut microbiota induce IGF-1 and promote bone formation and growth, Proc. Natl. Acad. Sci. U. S. A. 113 (2016) E7554–E7563, https://doi.org/10.1073/pnas.1607235113.
[20] T.C. Wallace, M. Marzorati, L. Spence, C.M. Weaver, P.S. Williamson, New Frontiers in fibers: innovative and emerging research on the gut microbiome and bone health, J. Am. Coll. Nutr. 36 (2017) 218–222, https://doi.org/10.1080/07315724.2016.1257961.
[21] S. Lucas, Y. Omata, J. Hofmann, M. Böttcher, A. Iljazovic, K. Sarter, O. Albrecht, O. Schulz, B. Krishnacoumar, G. Krönke, M. Herrmann, D. Mougiakakos, T. Strowig, G. Schett, M.M. Zaiss, Short-chain fatty acids regulate systemic bone mass and protect from pathological bone loss, Nat. Commun. 9 (2018) 55, , https://doi.org/10.1038/s41467-017-02490-4.
[22] C.M. Whisner, B.R. Martin, M.H. Schoterman, C.H. Nakatsu, L.D. McCabe, G.P. McCabe, M.E. Wastney, E.G. van den Heuvel, C.M. Weaver, Galacto-oligosaccharides increase calcium absorption and gut bifidobacteria in young girls: a double-blind cross-over trial, Br. J. Nutr. 110 (2013) 1292–1303, https://doi.org/10.1017/S000711451300055X.
[23] M.M. Rahman, A. Kukita, T. Kukita, T. Shobuike, T. Nakamura, O. Kohashi, Two histone deacetylase inhibitors, trichostatin a and sodium butyrate, suppress differentiation into osteoclasts but not into macrophages, Blood 101 (2003) 3451–3459, https://doi.org/10.1182/blood-2002-08-2622.
[24] T. Katono, T. Kawato, N. Tanabe, N. Suzuki, T. Iida, A. Morozumi, K. Ochiai, M. Maeno, Sodium butyrate stimulates mineralized nodule formation and osteoprotegerin expression by human osteoblasts, Arch. Oral Biol. 53 (2008) 903–909, https://doi.org/10.1016/j.archoralbio.2008.02.016.
[25] K.M. Maslowski, A.T. Vieira, A. Ng, J. Kranich, F. Sierro, D. Yu, H.C. Schilter, M.S. Rolph, F. Mackay, D. Artis, R.J. Xavier, M.M. Teixeira, C.R. Mackay, Regulation of inflammatory responses by gut microbiota and chemoattractant receptor GPR43, Nature 461 (2009) 1282–1286, https://doi.org/10.1038/nature08530.
[26] A.J. Brown, S.M. Goldsworthy, A.A. Barnes, M.M. Eilert, L. Tcheang, D. Daniels, A.I. Muir, M.J. Wigglesworth, I. Kinghorn, N.J. Fraser, N.B. Pike, J.C. Strum, K.M. Steplewski, P.R. Murdock, J.C. Holder, F.H. Marshall, P.G. Szekeres, S. Wilson, D.M. Ignar, S.M. Foord, A. Wise, S.J. Dowell, The orphan G protein-coupled receptors GPR41 and GPR43 are activated by propionate and other short chain carboxylic acids, J. Biol. Chem. 278 (2003) 11312–11319, https://doi.org/10.1074/jbc.M211609200.
[27] L. Macia, J. Tan, A.T. Vieira, K. Leach, D. Stanley, S. Luong, M. Maruya, C. Ian McKenzie, A. Hijikata, C. Wong, L. Binge, A.N. Thorburn, N. Chevalier, C. Ang, E. Marino, R. Robert, S. Offermanns, M.M. Teixeira, R.J. Moore, R.A. Flavell, S. Fagarasan, C.R. Mackay, Metabolite-sensing receptors GPR43 and GPR109A facilitate dietary fibre-induced gut homeostasis through regulation of the inflammasome, Nat. Commun. 6 (2015) 6734, , https://doi.org/10.1038/ncomms7734.
[28] W.R. Ribeiro, M.A. Vinolo, L.A. Calixto, C.M. Ferreira, Use of gas chromatography to quantify short chain fatty acids in the serum, colonic luminal content and feces of mice, Bio-protocol 8 (2018) 3089, , https://doi.org/10.21769/BioProtoc.3089.
[29] C.M. Weaver, B.R. Martin, J.A. Story, I. Hutchinson, L. Sanders, Novel fibers increase bone calcium content and strength beyond efficiency of large intestine fermentation, J. Agric. Food Chem. 58 (2010) 8952–8957, https://doi.org/10.1021/jf904086d.
[30] K.W. Oh, W.Y. Lee, E.J. Rhee, K.H. Baek, K.H. Yoon, M.I. Kang, E.J. Yun, C.Y. Park, S.H. Ihm, M.G. Choi, H.J. Yoo, S.W. Park, The relationship between serum resistin, leptin, adiponectin, ghrelin levels and bone mineral density in middle-aged men, Clin. Endocrinol. 63 (2005) 131–138, https://doi.org/10.1111/j.1365-2265.2005.02312.x.
[31] M.R. Sowers, R.P. Wildman, P. Mancuso, A.D. Eyvazzadeh, C.A. Karvonen-Gutierrez, E. Rillamas-Sun, M.L. Jannausch, Change in adipocytokines and ghrelin with menopause, Maturitas 59 (2008) 149–157, https://doi.org/10.1016/j.maturitas.2007.12.006.
[32] R. Axmann, C. Böhm, G. Krönke, J. Zwerina, J. Smolen, G. Schett, Inhibition of interleukin-6 receptor directly blocks osteoclast formation in vitro and in vivo, Arthritis Rheum. 60 (2009) 2747–2756, https://doi.org/10.1002/art.24781.
[33] X. Yang, B.F. Ricciardi, A. Hernandez-Soria, Y. Shi, N. Pleshko Camacho, M.P. Bostrom, Callus mineralization and maturation are delayed during fracture healing in interleukin-6 knockout mice, Bone 41 (2007) 928–936, https://doi.org/10.1016/j.bone.2007.07.022.
[34] M.D. Cantley, D.P. Fairlie, P.M. Bartold, K.D. Rainsford, G.T. Le, A.J. Lucke, C.A. Holding, D.R. Haynes, Inhibitors of histone deacetylases in class I and class II suppress human osteoclasts in vitro, J. Cell. Physiol. 226 (2011) 3233–3241, https://doi.org/10.1002/jcp.22684.
[35] N.G. Leus, P.E. van der Wouden, T. van den Bosch, W.T.R. Hooghiemstra, M.E. Ourailidou, L.E. Kistemaker, R. Bischoff, R. Gosens, H.J. Haisma, F.J. Dekker, HDAC 3-selective inhibitor RGFP966 demonstrates anti-inflammatory properties in RAW 264.7 macrophages and mouse precision-cut lung slices by attenuating NF-κB p65 transcriptional activity, Biochem. Pharmacol. 108 (2016) 58–74, https://doi.org/10.1016/j.bcp.2016.03.010.
[36] X.X. Chen, T. Yang, Roles of leptin in bone metabolism and bone diseases, J. Bone Miner. Metab. 33 (2015) 474–485, https://doi.org/10.1007/s00774-014-0569-7.
[37] J.J. Cao, B.R. Gregoire, C.L. Shen, A high-fat diet decreases bone mass in growing mice with systemic chronic inflammation induced by low-dose, slow-release lipopolysaccharide pellets, J. Nutr. 147 (2017) 1909–1916, https://doi.org/10.3945/jn.117.248302.